

## Article

# Synthesis, Structure and Properties of Polyester Polyureas via a Non-Isocyanate Route with Good Combined Properties

Liuchun Zheng <sup>1,2,3,\*</sup> , Qiqi Xie <sup>2</sup>, Guangjun Hu <sup>4</sup>, Bing Wang <sup>2</sup>, Danqing Song <sup>2</sup>, Yunchuan Zhang <sup>2</sup> and Yi Liu <sup>2</sup> <sup>1</sup> School of Chemical Engineering and Technology, Xinjiang University, Urumqi 830017, China<sup>2</sup> School of Chemical Engineering and Technology, State Key Laboratory of Separation Membranes and Membrane Processes, Education Ministry Key Laboratory of Hollow Fiber Membrane Materials and Membrane Processes, Tiangong University, Tianjin 300387, China<sup>3</sup> Cangzhou Insititute of Tiangong University, Cangzhou 061000, China<sup>4</sup> Shenghong Advanced Materials Research Institute, Shanghai 201403, China

\* Correspondence: liuchunzheng@tiangong.edu.cn or hubeizlc@126.com

**Abstract:** Polyureas have been widely applied in many fields, such as coatings, fibers, foams and dielectric materials. Traditionally, polyureas are prepared from isocyanates, which are highly toxic and harmful to humans and the environment. Synthesis of polyureas via non-isocyanate routes is green, environmentally friendly and sustainable. However, the application of non-isocyanate polyureas is quite restrained due to their brittleness as the result of the lack of a soft segment in their molecular blocks. To address this issue, we have prepared polyester polyureas via an isocyanate-free route and introduced polyester-based soft segments to improve their toughness and endow high impact resistance to the polyureas. In this paper, the soft segments of polyureas were synthesized by the esterification and polycondensation of dodecanedioic acid and 1,4-butanediol. Hard segments of polyureas were synthesized by melt polycondensation of urea and 1,10-diaminodecane without a catalyst or high pressure. A series of polyester polyureas were synthesized by the polycondensation of the soft and hard segments. These synthesized polyester-type polyureas exhibit excellent mechanical and thermal properties. Therefore, they have high potential to substitute traditional polyureas.

**Keywords:** non-isocyanate; polyurea; polyester; soft segment; impact resistance

**Citation:** Zheng, L.; Xie, Q.; Hu, G.; Wang, B.; Song, D.; Zhang, Y.; Liu, Y. Synthesis, Structure and Properties of Polyester Polyureas via a Non-Isocyanate Route with Good Combined Properties. *Polymers* **2024**, *16*, 993. <https://doi.org/10.3390/polym16070993>

Academic Editor: Valentina Siracusa

Received: 8 March 2024

Revised: 29 March 2024

Accepted: 2 April 2024

Published: 4 April 2024



**Copyright:** © 2024 by the authors. Licensee MDPI, Basel, Switzerland. This article is an open access article distributed under the terms and conditions of the Creative Commons Attribution (CC BY) license (<https://creativecommons.org/licenses/by/4.0/>).

## 1. Introduction

Polyurea is a kind of high-performance polymer material consisting of a urea group repeating unit with symmetric double-dentate hydrogen bonds [1]. Compared with single hydrogen-bonded polyamides and polyurethanes, double-dentate hydrogen bonds endow polyurea with a high crystallinity, melting point, rigidity and polarity [2]. As a result, polyurea possesses excellent tensile strength, heat resistance, bending resistance, corrosion resistance, solvent resistance and friction resistance. Therefore, polyurea has been widely applied in many fields, such as fibers, membranes, coatings and so on. In 2022, the global annual market value of polyurea reached \$885 million, and it is expected to reach \$1481 million by 2025 [3]. Polyureas are traditionally produced with diisocyanate (or polyisocyanate) and incorporate polyether or diamine as a chain extender. Isocyanates and their precursor, phosgene, are highly toxic and harmful to human health and the environment [4]. As isocyanate is also highly reactive, it is very hard to preserve and control its reaction [5]. In addition, it is a significant challenge to process polyureas because the melting temperature of polyureas with isocyanates is close to their decomposition temperature due to strong intermolecular hydrogen bonding [6].

To address the above issue, various methods have been tried to synthesize polyureas by non-isocyanate methods. Generally, non-isocyanate polyureas can be synthesized by carbon dioxide/diamine [7–13], carbamate/diamine [14–21] and urea/diamine reactions [1,5,22–26]. Shi et al. prepared polyureas with excellent mechanical and thermal

properties from carbon dioxide and diamines by a two-step process [8], but the reaction requires harsh conditions of high pressure, reaching as high as 11.5 MPa, which is potentially dangerous. Synthesis of polyureas from carbonate with diamines has attracted extensive attention. Kébir et al. synthesized polyureas with molecular weights ( $M_n$ ) ranging from  $1.7 \times 10^3$  to  $2.7 \times 10^3$  using dimethyl carbamates and various diamines as raw materials and 1,5,7-triazabicyclo [4.4.0]dec-5-ene as catalyst [14]. As the  $M_n$  is relatively low, the processing properties and mechanical properties of the polyureas are poor, and their application is greatly restrained. Li et al. synthesized thermoplastic polyureas with excellent mechanical properties from diethylene glycol bis(3-aminopropyl) ether, bis(hydroxyethyl) hexanediurethane and bis(hydroxyethyl) isophoronediuurethane by melt polycondensation [16]. However, the preparation process of intermediate product of bis(2-hydroxyethyl) diaminoate and dimethyl carbamates is complex and requires repeated purification, and the yield is relatively low. In contrast, the reaction conditions of polyureas from urea are mild, and do not require high pressure. Lin et al. produced biobased polyurea (PUr) from urea, biobased 1,6-diaminohexane (DA-6) and 1,10-diaminodecane (DA-10) [5]. The mechanical properties of PUr can be regulated by the feed ratio of DA-6 to DA-10. The results showed that PUr-6<sub>67</sub>10<sub>33</sub> exhibited a high tensile strength of 61 MPa and good elongation at break of 420%.

However, the chemical structure and properties of polyurea prepared by non-isocyanate methods differ significantly from those of polyurea prepared from isocyanate methods, which usually consists of two components, A and B. Component A is isocyanate or its prepolymer, and component B is the mixture of polyether amines, chain extenders and additives. The reaction of components A and B generates polyurea as a hard segment and polyether as a soft segment to endow the polymer with excellent mechanical properties [27]. The hard segments impart high modulus, strength and hardness to polyureas [28], while the soft ones provide toughness and impact resistance to polyureas [29]. Unfortunately, polyureas synthesized from non-isocyanate routes often lack soft segments. Consequently, they usually have shortcomings such as poor toughness and low impact resistance.

In this work, for the first time, we synthesized non-isocyanate polyureas with polyester as a soft segment. Firstly, urea and DA-10 were employed to synthesize polyureas prepolymer (Pre-PU) as the hard segment. Then, the soft segment, pre-polymerized poly(butylene dodecanedioate) (Pre-PBD), was synthesized by esterification and polycondensation of dodecanedioic acid (DDCA) and 1,4-butanediol (BDO). Finally, the polyester polyurea was synthesized through melt polycondensation of the soft segment and hard segment. The introduction of a soft segment largely improves the toughness and impact resistance of polyurea and expands its potential applications.

## 2. Materials and Methods

### 2.1. Materials

Urea (99.5%) and DA-10 (97%) were purchased from Macklin (Tianjing, China). DDCA with a purity of 99% was bought from Aladdin Biochemical Technology Co., Ltd. (Shanghai, China). The 1,4-butanediol (BDO) (99% purity) and stannous octoate ( $\text{Sn}(\text{Oct})_2$ , >96.0%) were purchased from J&K Chemical (Beijing, China). All the raw materials were used without further purification before the reaction.

### 2.2. Synthesis of Polyureas ( $\text{PBD}_x\text{PU}_y$ )

Polyurea was synthesized by the polycondensation of hard and soft segments. Pre-PU and Pre-PBD, corresponding to the hard and soft segments, were first synthesized, and then polycondensation was conducted to prepare a series of  $\text{PBD}_x\text{PU}_y$  with different mass ratios of Pre-PU to Pre-PBD. The polymerization and polycondensation processes are described as below.

### 2.2.1. Synthesis of Pre-PU

Pre-PU was synthesized via a three-step polycondensation method. Urea (1.6 mol, 96.10 g) and DA-10 (1.76 mol, 303.26 g) were fed to a 1 L kettle equipped with a nitrogen (N<sub>2</sub>) inlet and a fractionating column. The reactants were maintained at 130 °C for 2 h. Then, the temperature was raised to 210 °C and maintained for 1.5 h. Finally, the temperature was raised to 240 °C at 80 Pa for 20 min to obtain the Pre-PU.

<sup>1</sup>H NMR data (400 MHz, C<sub>2</sub>DF<sub>3</sub>O<sub>2</sub>-d<sub>1</sub>, δ in ppm): 3.35-3.24 (a, -CH<sub>2</sub>NH-), 3.24-3.15 (f, -CH<sub>2</sub>NH<sub>2</sub>), 1.79-1.68 (g, -CH<sub>2</sub>CH<sub>2</sub>NH-), 1.67-1.54 (h, -CH<sub>2</sub>CH<sub>2</sub>NH-), 1.44-1.21 (c, d, e, -CH<sub>2</sub>CH<sub>2</sub>CH<sub>2</sub>CH<sub>2</sub>CH<sub>2</sub>NH-).

### 2.2.2. Synthesis of Pre-PBD

Pre-PBD was synthesized through a two-step reaction involving esterification and polycondensation. DDCA (1.2 mol, 272.36 g) and BDO (1.44 mol, 129.60 g) were fed into a 1 L kettle. The reaction system was heated to 160 °C under stirring with the protection of N<sub>2</sub>. Then, Sn(Oct)<sub>2</sub> (0.0804 g, 0.02 wt%) was added as a catalyst. The esterification then proceeded until the esterification yield reached 90%. Then, the temperature was raised to 230 °C and the system pressure was reduced to 80 Pa for 0.8 h. The product was cooled by water and cut into pellets.

<sup>1</sup>H NMR data (400 MHz, C<sub>2</sub>DF<sub>3</sub>O<sub>2</sub>-d<sub>1</sub>, δ in ppm): 4.23-4.10 (a, -CH<sub>2</sub>C(O)OCH<sub>2</sub>-), 2.42-2.30 (b, -CH<sub>2</sub>C(O)OCH<sub>2</sub>-), 1.89-1.81 (c, -CH<sub>2</sub>CH<sub>2</sub>CH<sub>2</sub>OH), 1.80-1.67 (d, -CH<sub>2</sub>C(O)OCH<sub>2</sub>CH<sub>2</sub>-), 1.67-1.50 (e, -CH<sub>2</sub>CH<sub>2</sub>C(O)OCH<sub>2</sub>-), 1.35-1.14 (f, -CH<sub>2</sub>CH<sub>2</sub>CH<sub>2</sub>CH<sub>2</sub>CH<sub>2</sub>C(O)OCH<sub>2</sub>-).

<sup>1</sup>H NMR data (400 MHz, CDCl<sub>3</sub>-d<sub>1</sub>, δ in ppm): 4.12-4.04 (a, -CH<sub>2</sub>C(O)OCH<sub>2</sub>-), 3.69-3.65 (b, -CH<sub>2</sub>OH), 2.34-2.21 (c, -CH<sub>2</sub>CH<sub>2</sub>C(O)OCH<sub>2</sub>-), 1.71-1.65 (d, -CH<sub>2</sub>C(O)OCH<sub>2</sub>CH<sub>2</sub>-), 1.64-1.55 (e, -CH<sub>2</sub>CH<sub>2</sub>C(O)OCH<sub>2</sub>-), 1.34-1.22 (f, -CH<sub>2</sub>CH<sub>2</sub>CH<sub>2</sub>CH<sub>2</sub>CH<sub>2</sub>C(O)O-).

### 2.2.3. Synthesis of PBD<sub>x</sub>PU<sub>y</sub>

A typical procedure for preparing PBD<sub>x</sub>PU<sub>y</sub> is described below: predetermined amounts of Pre-PBD and Pre-PU were added to a kettle equipped with a nitrogen inlet and a fractionating column and stirred at 230 °C under the pressure of 80 Pa for 1–3 h. In order to obtain polymers with similar molecular weight, the polycondensation process continued until the torque reach a fixed value (5.5 N·m). For PBD<sub>x</sub>PU<sub>y</sub>, x and y represent the mass fraction of Pre-PBD and Pre-PU, respectively. For example, PBD<sub>70%</sub>PU<sub>30%</sub> means the sample whose mass ratios of Pre-PBD and Pre-PU are 70% and 30%, respectively. The prepared samples are named as PBD<sub>80%</sub>PU<sub>20%</sub>, PBD<sub>70%</sub>PU<sub>30%</sub>, PBD<sub>60%</sub>PU<sub>40%</sub> and PBD<sub>50%</sub>PU<sub>50%</sub>.

<sup>1</sup>H NMR data (400 MHz, C<sub>2</sub>DF<sub>3</sub>O<sub>2</sub>-d<sub>1</sub>, δ in ppm): 4.28-4.10 (a, -CH<sub>2</sub>C(O)OCH<sub>2</sub>-), 3.53-3.42 (d, -CH<sub>2</sub>NHC(O)CH<sub>2</sub>-), 3.36-3.18 (c, -CH<sub>2</sub>NHC(O)NHCH<sub>2</sub>-), 2.71-2.59 (b, -CH<sub>2</sub>NHC(O)CH<sub>2</sub>-), 2.48-2.28 (e, -CH<sub>2</sub>C(O)OCH<sub>2</sub>-), 1.82-1.67 (f, -CH<sub>2</sub>CH<sub>2</sub>O(O)CCH<sub>2</sub>CH<sub>2</sub>-), 1.62-1.52 (g, -CH<sub>2</sub>CH<sub>2</sub>CH<sub>2</sub>C(O)OCH<sub>2</sub>CH<sub>2</sub>CH<sub>2</sub>- and -CH<sub>2</sub>CH<sub>2</sub>NHC(O)NHCH<sub>2</sub>CH<sub>2</sub>-), 1.40-1.12 (h, -CH<sub>2</sub>CH<sub>2</sub>CH<sub>2</sub>CH<sub>2</sub>CH<sub>2</sub>C(O)OCH<sub>2</sub>- and -CH<sub>2</sub>CH<sub>2</sub>CH<sub>2</sub>CH<sub>2</sub>CH<sub>2</sub>NHC(O)NH-).

### 2.3. Characterizations

The synthesized Pre-PBD, Pre-PU and polyurea were characterized by <sup>1</sup>H NMR and FT-IR spectroscopy. <sup>1</sup>H-NMR spectra were obtained using a Bruker A VIII600 NMR spectrometer at 25 °C (500 MHz, Bruker BioSpin Co., Ettlingen, Germany). The solvents were deuterated chloroform (CDCl<sub>3</sub>) or deuterated trifluoroacetic acid (C<sub>2</sub>DF<sub>3</sub>O<sub>2</sub>). An FTIR spectrometer (Varian 640-IR, Varian, Sydney, Australia) was used to test the FTIR spectra of samples, and the scan range was 4000 to 400 cm<sup>-1</sup>.

Thermal properties were measured using differential scanning calorimetry (DSC) (DSC-Q5800, Perkin-Elmer Co., Waltham, MA, USA). A sample of approximately 5–10 mg was placed in an aluminum crucible and scanned from 50 °C to 250 °C at 10 °C/min and kept there for 10 min under high-purity N<sub>2</sub> to remove thermal history. Then, the sample was cooled to -25 °C at 100 °C/min and kept there for 10 min, and subsequently reheated to 250 °C at a rate of 10 °C/min. After maintaining at 250 °C for 5 min, the sample was

then cooled to  $-25\text{ }^{\circ}\text{C}$  at a rate of  $10\text{ }^{\circ}\text{C}/\text{min}$ . Both heating and cooling curves were recorded. The thermal stability of  $\text{PBD}_x\text{PU}_y$  was tested on a thermogravimetric analyser (TGA) (NETZSCH TG 209 F3, Selb, Germany). The samples were heated at a rate of  $20\text{ }^{\circ}\text{C}/\text{min}$  from  $50\text{ }^{\circ}\text{C}$  to  $800\text{ }^{\circ}\text{C}$  under an  $\text{N}_2$  atmosphere. Dynamic mechanical analysis (DMA) of  $\text{PBD}_x\text{PU}_y$  was performed using a DMA242E (Netzsch Co., Selb, Germany). It was conducted in shear mode, using a temperature sweeping from  $-90\text{ }^{\circ}\text{C}$  to  $40\text{ }^{\circ}\text{C}$ , with a heating rate of  $5\text{ }^{\circ}\text{C}/\text{min}$ .

Wide angle X-ray analysis (WAXD) was conducted using an X-ray diffractometer (Bruker D8 DISCOVER, German Bruker company, Karlsruhe, Germany). The samples were scanned from  $7^{\circ}$  to  $45^{\circ}$  at a scanning speed of  $2^{\circ}/\text{min}$  using a  $\text{Cu K}\alpha$  radiation ( $\lambda = 154\text{ nm}$ ) target.

In order to explore the mechanical properties of  $\text{PBD}_x\text{PU}_y$ , PBD and PU, tensile properties, flexural properties and impact properties were studied. The tensile testing of dumbbell-shaped samples ( $80.0\text{ mm} \times 5.0\text{ mm} \times 2.0\text{ mm}$ ) was performed on an Instron 1122 tensile tester according to ISO 527 [30]. The crosshead speed was  $50\text{ mm}/\text{min}$ . The flexural testing of samples ( $80.0\text{ mm} \times 10.0\text{ mm} \times 4.0\text{ mm}$ ) was conducted on the same equipment according to ISO 178 [31], and the bending modulus was calculated from the slope of the stress-strain curve in the strain range of 0~1%. V-Notch impact strength testing of samples ( $80.0\text{ mm} \times 10.0\text{ mm} \times 4.0\text{ mm}$ ) was performed on a pendulum impact tester (Shenzhen Sansi Co., Shenzhen, China) according to ISO 179 [32]. At least five specimens were tested for each sample, and the average value was reported.

The fracture surfaces of samples were coated with gold. Then, they were characterized using a scanning electron microscope (MERLIN Compact, Zeiss, Oberkochen, Germany) with an accelerating voltage of  $15\text{ kV}$ .

### 3. Results and Discussion

#### 3.1. Chemical Structure Characterization of $\text{PBD}_x\text{PU}_y$

The synthesis route of  $\text{PBD}_x\text{PU}_y$  is illustrated in Figure 1.  $\text{PBD}_x\text{PU}_y$  was synthesized by polycondensation of Pre-PBD and Pre-PU. The average molecular weights of Pre-PBD and Pre-PU, calculated from the  $^1\text{H NMR}$  data using the equations provided in the literature, are  $5600\text{ g}/\text{mol}$  and  $1700\text{ g}/\text{mol}$ , respectively [8,33]. The  $^1\text{H NMR}$  spectra of  $\text{PBD}_x\text{PU}_y$  are shown in Figure 2. The integral area of new peaks at  $2.64\text{ ppm}$  (b) and  $3.48\text{ ppm}$  (d) in Figure 2b, attributed to the hydrogens on an  $\alpha$ -carbon atom attached to the carbonyl and amine of the amide bond, respectively [34], is the same. It can be found that with the decrease of Pre-PBD content, the integral area of hydrogen at  $4.18\text{ ppm}$  (a) of the  $\alpha$ -carbon attached to the oxygen atom of ester decreased and the integral area of hydrogen at  $3.24\text{ ppm}$  (c) of the  $\alpha$ -carbon attached to nitrogen atom in the urea group increased, indicating that the content of the ester group decreased and the content of the urea group increased. This demonstrates that  $\text{PBD}_x\text{PU}_y$  had been successfully synthesized. However,  $\text{PBD}_x\text{PU}_y$  could not be completely dissolved in TFA. Therefore, it is challenging to calculate the number average molecular weight of  $\text{PBD}_x\text{PU}_y$  using  $^1\text{H NMR}$  data.

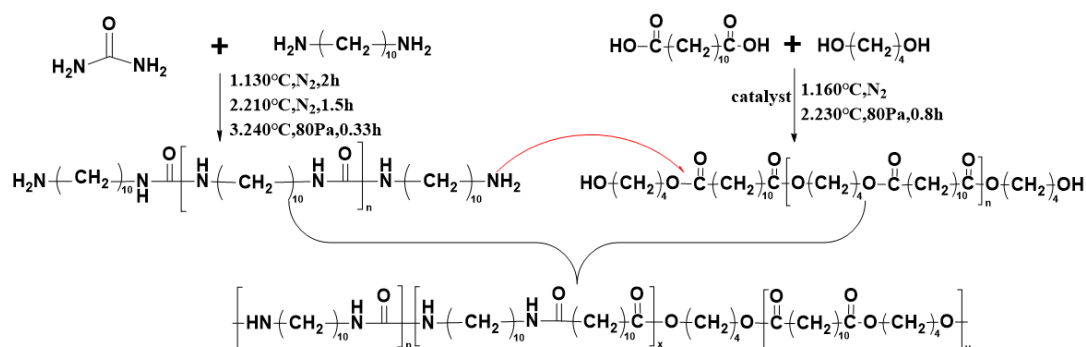
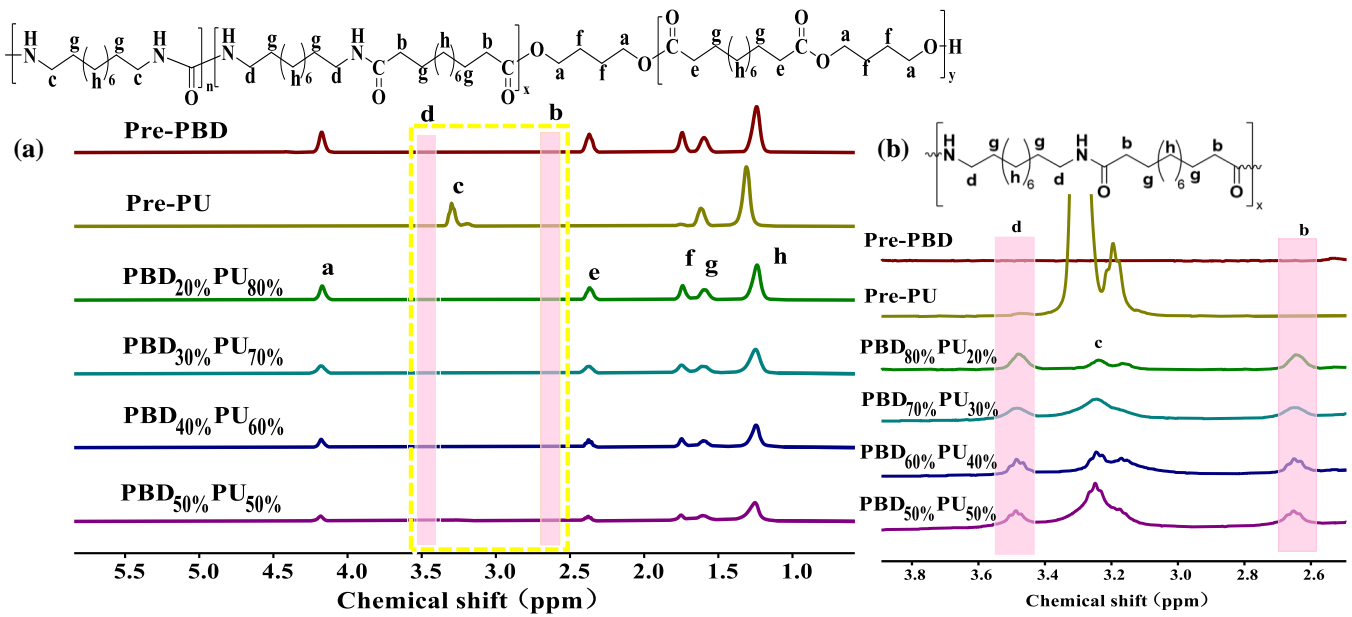
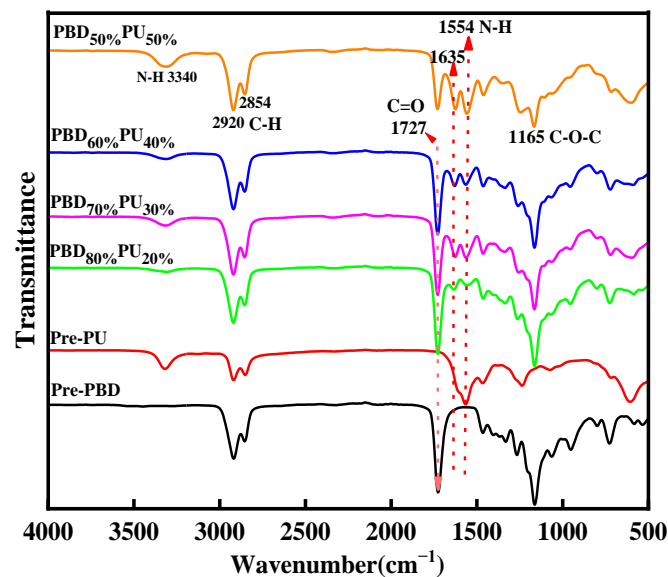


Figure 1. Synthesis route of  $\text{PBD}_x\text{PU}_y$ .



**Figure 2.**  $^1\text{H}$  NMR spectra of  $\text{PBD}_x\text{PU}_y$  (Pre-PBD and Pre-PU): (a) the full spectra. (b) partially enlarged spectra.

The chemical structure of Pre-PBD, Pre-PU and  $\text{PBD}_x\text{PU}_y$  was further studied by FTIR spectra. Figure 3 shows the FTIR spectra of the prepolymer and polyureas. As shown in Figure 3, the stretching vibration peak of the amino group is observed at  $3340\text{ cm}^{-1}$ , while the stretching vibration peak of methylene group is found in the range of  $2920\text{--}2854\text{ cm}^{-1}$ . The bending vibration peak of the amino group appears at  $1554\text{ cm}^{-1}$ . Additionally, the asymmetric stretching vibration peak of the C-O-C ether bond is observed at  $1165\text{ cm}^{-1}$ , and the peak at  $1727\text{ cm}^{-1}$  corresponds to the stretching vibration of the carbonyl group in the ester group. The stretching vibration peak of the carbonyl group in the urea group is observed at  $1635\text{ cm}^{-1}$ . Both  $^1\text{H}$  NMR hydrogen spectra and the FTIR spectra confirmed that the resulting polymers were our target products.



**Figure 3.** FTIR spectra of Pre-PBD, Pre-PU and  $\text{PBD}_x\text{PU}_y$ . The arrows in the diagram are used to indicate the wavenumbers and corresponding function groups.

Many papers have shown that the carbonyl area also provides detailed information on hydrogen bonding. To further analyze the hydrogen bonding of polyureas, the carbonyl peaks of PBD<sub>x</sub>PU<sub>y</sub> were differentiated and fitted using Peak Fit v4.12 software. The maximum error of the fitting was less than 0.5%, and the correlation coefficient was higher than 0.995. The results of fitting curves of FTIR spectra for PBD<sub>x</sub>PU<sub>y</sub> are presented in Figure 4 and Table 1. As shown in Figure 4, the carbonyl stretching region of PBD<sub>x</sub>PU<sub>y</sub> is divided into five Gaussian peaks [35]. Peaks at 1628 cm<sup>-1</sup> and 1653 cm<sup>-1</sup> are attributed to the hydrogen bonded urea carbonyl groups in the disordered and ordered phase, respectively. The peak at 1691 cm<sup>-1</sup> is attributed to the free urea carbonyl. The peaks at 1674 cm<sup>-1</sup> and 1728 cm<sup>-1</sup> are ascribed to the free and hydrogen-bonded ester carbonyl groups, respectively. The peak percentage areas are listed in Table 1. The proportion of hydrogen-bonded ester carbonyl group in PBD<sub>70%</sub>PU<sub>30%</sub> is only 4.96%, while it reaches 17.06% for PBD<sub>50%</sub>PU<sub>50%</sub>, indicating the increasing interaction between the soft and hard segments with the increase of PU content. The hydrogen bonding interactions between soft and hard segments could significantly affect the thermal properties, crystallization and mechanical properties of the material, which will be discussed later.

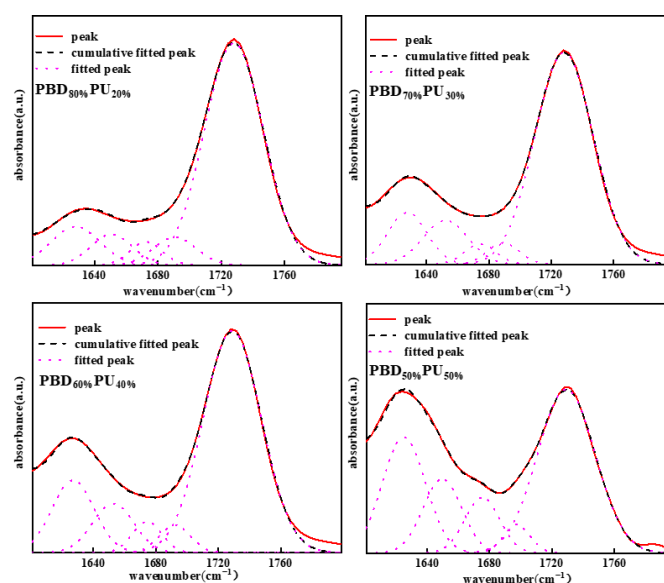


Figure 4. Fitting curves of FTIR spectra of PBD<sub>x</sub>PU<sub>y</sub>.

Table 1. Calculated relevant parameters from FTIR-fitting results.

	PBD <sub>80%</sub> PU <sub>20%</sub>	PBD <sub>70%</sub> PU <sub>30%</sub>	PBD <sub>60%</sub> PU <sub>40%</sub>	PBD <sub>50%</sub> PU <sub>50%</sub>
1626–1628 urea (bonded, ordered) A <sub>1</sub>	10.34%	11.51%	15.48%	25.03%
1652–1654 urea (bonded disordered) A <sub>2</sub>	7.00%	11.11%	10.25%	14.34%
1690–1691 urea (free) A <sub>3</sub>	6.54%	3.89%	4.33%	3.76%
1672–1674 ester (bonded) A <sub>4</sub>	4.10%	3.6%	4.63%	9.70%
1728–1729 ester (free) A <sub>5</sub>	72.05%	79.90%	65.31%	47.16%
(A <sub>1</sub> + A <sub>2</sub> )/(A <sub>1</sub> + A <sub>2</sub> + A <sub>3</sub> )	72.57%	85.34%	85.59%	91.28%
A <sub>4</sub> /(A <sub>4</sub> + A <sub>5</sub> )	5.38%	4.90%	6.61%	17.06%

### 3.2. Thermal Properties of PBD<sub>x</sub>PU<sub>y</sub>

Thermal properties are very important for polymer materials when it comes to application. Therefore, the thermal properties of PBD<sub>x</sub>PU<sub>y</sub> were studied by DSC and the results are shown in Figure 5. Only PBD<sub>50%</sub>PU<sub>50%</sub> did not show a melting peak of its soft segment, due to its high content of urea groups, which are capable of forming extensive hydrogen bonding with soft segments and reducing the crystallinity of soft segments, making it difficult for the material to fold into a regular crystal. All other PBD<sub>x</sub>PU<sub>y</sub> samples exhibit two distinct melting peaks, corresponding to the melting of the polyester soft segment and polyurea hard segment in the polymer. It should be noted that hard segment of PBD<sub>50%</sub>PU<sub>50%</sub> has two melting peaks, while the hard segments of other PBD<sub>x</sub>PU<sub>y</sub> only have one. This could be due to the fact that a polyurea with a different degree of polymerization of its hard segment was formed for PBD<sub>50%</sub>PU<sub>50%</sub> due to the self-condensation of the Pre-PU that occurs when the soft segment content is relatively low. The melting point of the hard segment is primarily influenced by two factors: degree of polymerization and hydrogen bonding. A higher degree of polymerization of the macromolecular chain leads to a higher melting point. The strong hydrogen bonding interaction between two segments not only results in decreased crystallinity and folding ability of the hard and soft segments, but also restricts the mobility of both segments. As a result, the melting point of the hard segment decreases. As shown in Table 2, the melting point of the soft and hard segments of PBD<sub>70%</sub>PU<sub>30%</sub> is higher than that of PBD<sub>80%</sub>PU<sub>20%</sub>, which can be attributed to the higher molar content of the polyurea hard segment of PBD<sub>70%</sub>PU<sub>30%</sub>. The hydrogen bonding of the hard segments of PBD<sub>70%</sub>PU<sub>30%</sub> is higher than that of PBD<sub>80%</sub>PU<sub>20%</sub>, but the interaction between the soft segment and hard segment for PBD<sub>70%</sub>PU<sub>30%</sub> is lower than that of PBD<sub>20%</sub>PU<sub>80%</sub>. Thus, the melting points of both the soft segment and hard segment increase. However, with further increases of polyurea hard segment content, the melting points of both the soft segment and hard segment decrease. PBD<sub>60%</sub>PU<sub>40%</sub> shows lower melting points of the soft and hard segments than those of PBD<sub>70%</sub>PU<sub>30%</sub>, which could be ascribed to the larger amount of hydrogen bonds formed between the soft and hard segments in PBD<sub>60%</sub>PU<sub>40%</sub>, as a higher content of hard segment is introduced. These hydrogen bonds restrict chain folding and decrease the crystallization ability of the soft and hard segments, leading to the decreases of their melting points. Furthermore, the melting peak of the hard segment of PBD<sub>60%</sub>PU<sub>40%</sub> becomes wider and the area becomes larger as the polyurea content increases, implying a higher crystallinity of the hard segment. This is due to the self-polycondensation of the hard segment of PBD<sub>x</sub>PU<sub>y</sub>. Due to the same reason, different lengths of hard segment have been formed, resulting in the two  $T_{m2}$  of PBD<sub>50%</sub>PU<sub>50%</sub>. As the melting point of the hard segment is above 180 °C, it can be concluded that the newly synthesized PBD<sub>x</sub>PU<sub>y</sub> has a relatively high melting point.

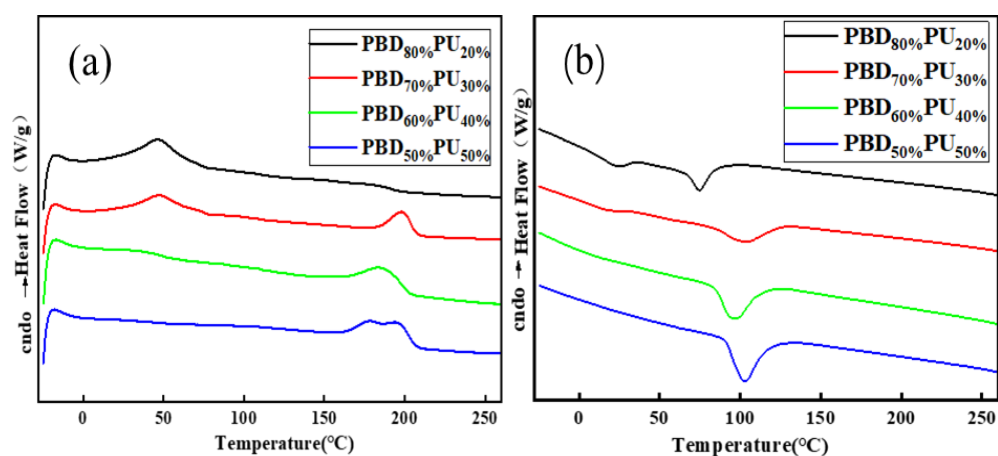
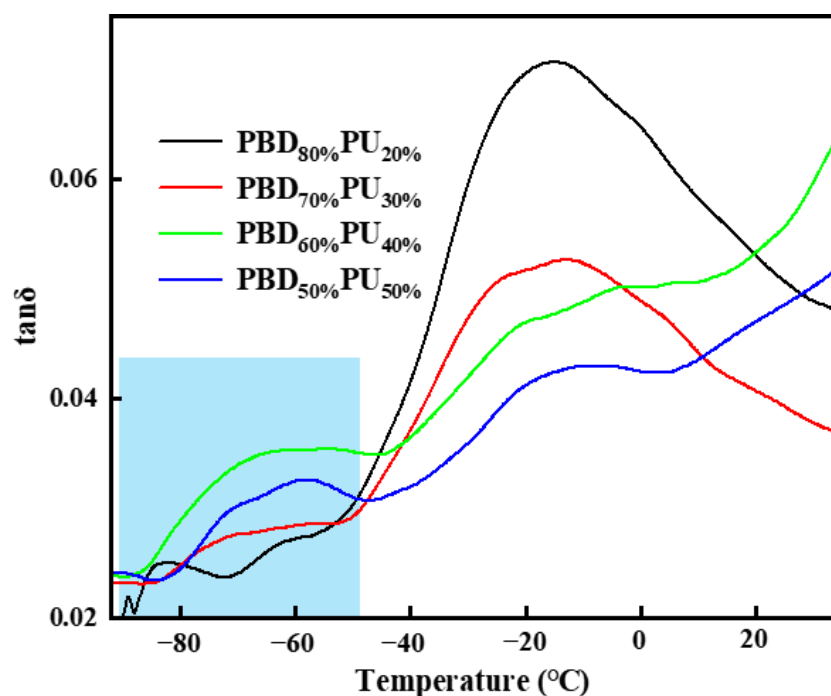


Figure 5. DSC of PBD<sub>x</sub>PU<sub>y</sub>: second heating (a) and cooling scans (b).

**Table 2.** Thermal performance parameters of PBD<sub>x</sub>PU<sub>y</sub>.

	$T_{m1}$ (°C)	$\Delta H_m$ (J/g)	$T_{m2}$ (°C)	$\Delta H_m$ (J/g)	$T_{c1}$ (°C)	$T_{c2}$ (°C)	$T_g$ (°C)	
							$\beta$	$\alpha$
PBD <sub>80%</sub> PU <sub>20%</sub>	46.5	25.7	179.3	3.4	24.1	74.5	−60.5	−15.3
PBD <sub>70%</sub> PU <sub>30%</sub>	47.4	17.7	198.2	9.7	16.9	102.8	−64.9	−13.7
PBD <sub>60%</sub> PU <sub>40%</sub>	36.7	3.3	188.2	17.5	-	95.9	−59.2	−3.6
PBD <sub>50%</sub> PU <sub>50%</sub>	-	-	180.0, 194.7	21.0	-	102.6	−62.7	−11.2

DMA is more sensitive to the movement of macromolecular chains, and Figure 6 shows the  $\tan \delta$  versus temperature curves of PBD<sub>x</sub>PU<sub>y</sub>. It can be observed from Figure 6 that PBD<sub>x</sub>PU<sub>y</sub> exhibits two glass transition temperatures ( $T_g$ ) ranging from  $-80$  °C to  $0$  °C, suggesting it possesses excellent toughness at low temperatures. For  $T_g$  in the range of  $-40$  °C to  $0$  °C, the motion of the polyester soft segments is referred to as the  $\alpha$  transition or micro-Brownian chain motion. Sub- $T_g$ , in the temperature range of  $-50$  °C to  $-80$  °C, is related to the  $\beta$  transition, corresponding to the localized chains or small unit motion [36]. For the  $\beta$  transition, the peak intensity and width of PBD<sub>50%</sub>PU<sub>50%</sub> and PBD<sub>60%</sub>PU<sub>40%</sub> increase compared to PBD<sub>80%</sub>PU<sub>20%</sub>, suggesting that the number of the small units that can mobilize increases. This phenomenon may occur because more of the soft segments in the polyureas cannot crystallize due to hydrogen bonding, which leads to the decreased crystallizability of the polyureas, resulting in the fact that the number of movable groups and units in the amorphous region increases.

**Figure 6.**  $\tan \delta$  versus temperature for PBD<sub>x</sub>PU<sub>y</sub>.

### 3.3. Thermal Stability of PBD<sub>x</sub>PU<sub>y</sub>

The thermal stability and  $T_m$  of polymers determine their processability. Figure 7 displays the curves of thermogravimetric analysis (TGA) and derivative thermogravimetry (DTG) for PBD<sub>x</sub>PU<sub>y</sub>. It can be found from Figure 7 that the TGA and DTG curves of PBD<sub>x</sub>PU<sub>y</sub> exhibit similar shapes, suggesting that the synthesized polymers have similar thermal decomposition mechanisms. Moreover, all PBD<sub>x</sub>PU<sub>y</sub> have initial decomposition temperatures ( $T_{5\%}$ ) higher than  $316$  °C, suggesting that the synthesized PBD<sub>x</sub>PU<sub>y</sub> samples possess excellent thermal stabilities. The thermal decomposition behaviors of the polymers can be analyzed through the DTG curves, which shows a three-stage degradation process:

the initial maximum decomposition rate at 351 °C, which can be interpreted as the breakage of C-N bond in urea group [5], the second stage of decomposition, which its maximum decomposition rate at 415 °C due to the breakage of ester groups [34] and the third maximum decomposition rate occurs at 450 °C, which is caused by the destruction of the long carbon chains. Table 3 shows the main degradation temperatures of PBD<sub>x</sub>PU<sub>y</sub>. All  $T_{5\%}$  (>316 °C) of PBD<sub>x</sub>PU<sub>y</sub> are evidently higher than the  $T_m$  (198 °C), implying that they have good thermal stability during processing and their processing-temperature range is wide.

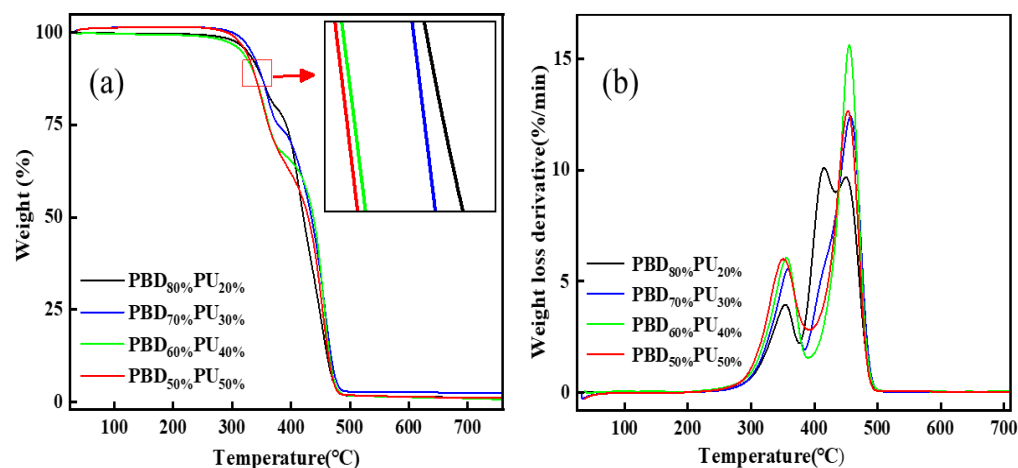


Figure 7. TGA curves (a) and DTG curves (b) for PBD<sub>x</sub>PU<sub>y</sub>.

Table 3. Main degradation temperatures of PBD<sub>x</sub>PU<sub>y</sub>.

	$T_{5\%}$ (°C)	$T_{max1}$ (°C)	$T_{max2}$ (°C)	$T_{max3}$ (°C)
PBD <sub>80%</sub> PU <sub>20%</sub>	320	354	415	450
PBD <sub>70%</sub> PU <sub>30%</sub>	316	358	416	457
PBD <sub>60%</sub> PU <sub>40%</sub>	331	356	-	455
PBD <sub>50%</sub> PU <sub>50%</sub>	325	351	-	453

### 3.4. Crystallization Properties of PBD<sub>x</sub>PU<sub>y</sub> Films

The WAXD diffraction pattern was used to further analyze the crystalline properties of PBD<sub>x</sub>PU<sub>y</sub> and the results are shown in Figure 8. Two distinct peaks with  $2\theta$  values at 21.22° and 23.56° can be observed for PBD<sub>80%</sub>PU<sub>20%</sub> and PBD<sub>70%</sub>PU<sub>30%</sub>, which are almost identical to the diffraction peaks of PBD as previously reported in the literature ( $2\theta = 21.39^\circ$  and  $23.72^\circ$ ) [37]. This suggests that the polyester soft segment in the polymer is highly crystallized. To further analyze the crystallinity of PBD<sub>x</sub>PU<sub>y</sub>, the WAXD peaks of PBD<sub>x</sub>PU<sub>y</sub> were differentiated and fitted using Peak Fit v4.12 software. The peaks of WAXD spectra of all four samples can be divided into four Gaussian-fitted peaks (21.39°, 23.72°, 20.60°, 22.70°) according to the literature [5,37], as shown in Figure 9. The maximum fitting error was less than 0.5% and the correlation coefficient was all greater than 0.995. The crystallinity was calculated and is listed in Table 4. PBD<sub>50%</sub>PU<sub>50%</sub> shows a wide and small peak, suggesting a low crystallinity of its soft segment. This could be attributed to its low content and the strong intermolecular hydrogen bonding between the polyurea hard segment and polyester soft segment. This is consistent with the DSC results. For DSC curves, there is no melting peak for the soft segment of PBD<sub>50%</sub>PU<sub>50%</sub> seen in the DSC. Due to the poor crystallization ability of PBD<sub>50%</sub>PU<sub>50%</sub>, it has an elongation at break as high as 135.0%, which will be discussed later. Both the WAXD and DSC of all samples, except for PBD<sub>70%</sub>PU<sub>30%</sub>, testified that the crystallinity of polyester soft segments reduces with decreasing content of Pre-PBD.

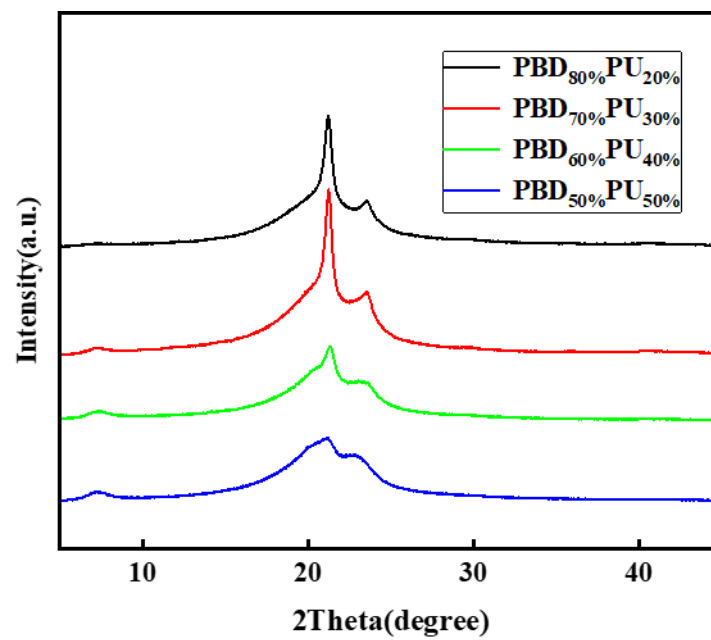


Figure 8. WAXD diffraction pattern of  $PBD_xPU_y$  films.

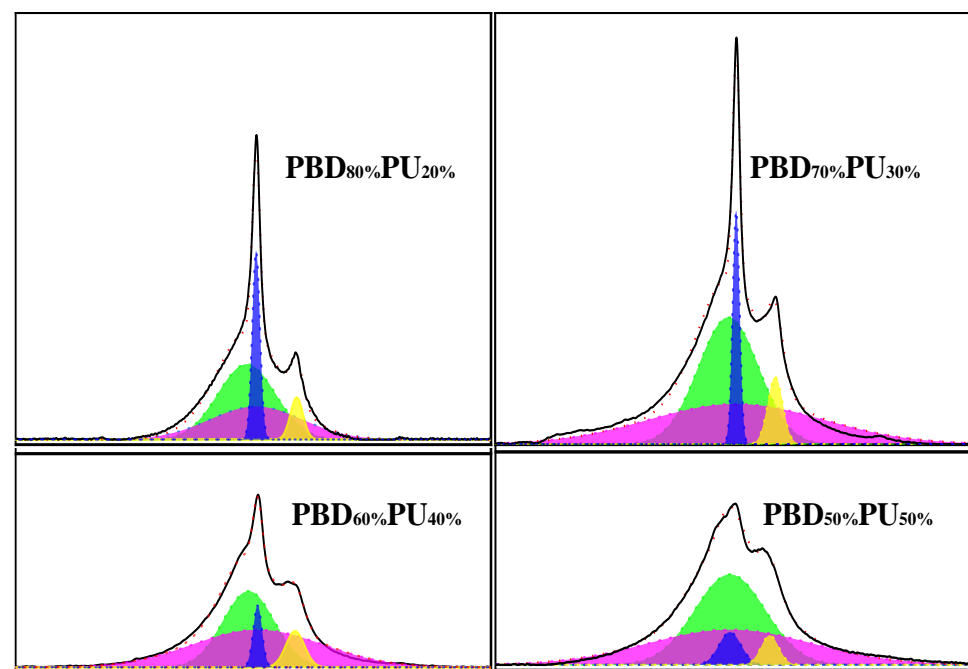


Figure 9. Fitting curves of WAXD diffraction pattern of  $PBD_xPU_y$ .

Table 4. Crystallinity of  $PBD_xPU_y$ .

Property	PBD <sub>80%</sub> PU <sub>20%</sub>	PBD <sub>70%</sub> PU <sub>30%</sub>	PBD <sub>60%</sub> PU <sub>40%</sub>	PBD <sub>50%</sub> PU <sub>50%</sub>
Crystallinity (%)	15.70	18.55	12.33	9.29

### 3.5. Mechanical Properties of $PBD_xPU_y$

The mechanical properties of polymers are very important for polymer materials when come to applications. Figure 10 displays the tensile curves of  $PBD_xPU_y$ , while Table 5 summarizes the mechanical property data of  $PBD_xPU_y$ . It can be found that the tensile

strength of PBD<sub>x</sub>PU<sub>y</sub> increases with the content of Pre-PU. The highest tensile strength of 46.1 MPa is observed when the mass content of Pre-PU is 50%. This can be attributed to the higher content of double-dentate hydrogen bonding between the polyurea hard segment that enhances the tensile strength of the polymer. PBD<sub>80%</sub>PU<sub>20%</sub> demonstrates the highest elongation at break of 197.8%, which could be explained by the fact that a high Pre-PBD soft segment content endows good toughness of the polyurea. It should be noted that the elongation at break of PBD<sub>50%</sub>PU<sub>50%</sub> is 135.0%, which is higher than that of PBD<sub>70%</sub>PU<sub>30%</sub> and PBD<sub>60%</sub>PU<sub>40%</sub>. This is due to fact that the content of Pre-PU is higher in PBD<sub>50%</sub>PU<sub>50%</sub>, which leads to more hydrogen bonding between the soft and hard segments, restricting the macromolecular chain folding and decreasing the crystallization of the soft segment. Previous DSC and WAXD results also indicate the same. It should be noted that the flexural strength, flexural modulus and impact strength of PBD<sub>x</sub>PU<sub>y</sub> also increase with increasing Pre-PU content. The impact strength of PBD<sub>50%</sub>PU<sub>50%</sub> can reach as high as 37.2 kJ/m<sup>2</sup> for PBD<sub>50%</sub>PU<sub>50%</sub>, which is enhanced by about four times as compared to PBD<sub>80%</sub>PU<sub>20%</sub> or PU-10. This is due to the fact that with the increase of Pre-PU content, the amount of the hydrogen bonding between the hard and soft segments increases substantially and the crystallinity of the soft segment in the PBD<sub>50%</sub>PU<sub>50%</sub> reduces significantly. This improves the toughness and impact resistance of PBD<sub>50%</sub>PU<sub>50%</sub>. The polymer not only exhibits good toughness, but also possesses high strength and modulus. Therefore, it can be safely concluded that the synthesized polyureas have good combined mechanical properties.

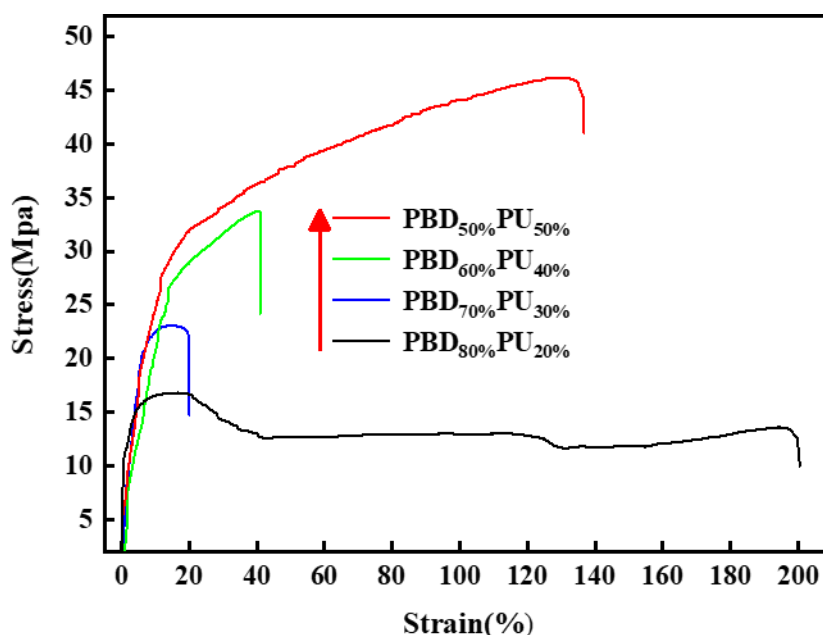


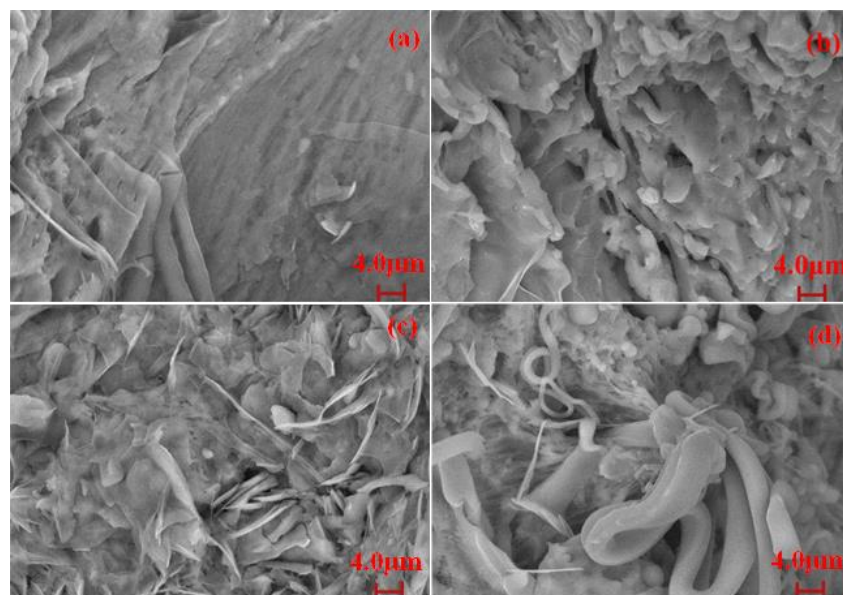
Figure 10. Stress-strain curves of PBD<sub>x</sub>PU<sub>y</sub>.

Table 5. Mechanical properties of PBD<sub>x</sub>PU<sub>y</sub>.

Sample	Impact Strength kJ/m <sup>2</sup>	Tensile Strength MPa	Elongation at Breaking%	Flexural Modulus MPa	Flexural Strength MPa
PBD <sub>80%</sub> PU <sub>20%</sub>	7.5	16.5	197.8	269.0	9.8
PBD <sub>70%</sub> PU <sub>30%</sub>	24.5	23.0	18.2	423.1	14.8
PBD <sub>60%</sub> PU <sub>40%</sub>	31.1	33.6	41.4	456.4	15.6
PBD <sub>50%</sub> PU <sub>50%</sub>	37.2	46.1	135.0	524.6	18.6
PBD	30.0	13.0	380.1	500.4	16.2
PU-10	6.8	70.0	24.0	1402.7	48.8

### 3.6. Morphology of $PBD_xPU_y$

The cross-section morphologies of different polymers were observed by SEM to analyze their fracture behaviors. The SEM images of the fracture of  $PBD_xPU_y$  are displayed in Figure 11. It can be observed that fracture surface of  $PBD_xPU_y$  is rough, which indicates a tough nature. Therefore,  $PBD_xPU_y$  possesses high impact resistance, which has been also indicated by the results shown in Table 5. The fracture surfaces of  $PBD_{80\%}PU_{20\%}$  appear relatively smooth, while  $PBD_{60\%}PU_{40\%}$  and  $PBD_{50\%}PU_{50\%}$  display a relatively rough surface with more pits. It should be noted that a myriad of fibrillation and fiber pulling-out phenomena occurred for  $PBD_{50\%}PU_{50\%}$ , which is the reason for its good toughness.



**Figure 11.** SEM images of quenched section of (a)  $PBD_{80\%}PU_{20\%}$ , (b)  $PBD_{70\%}PU_{30\%}$ , (c)  $PBD_{60\%}PU_{40\%}$ , (d)  $PBD_{50\%}PU_{50\%}$ .

## 4. Conclusions

In this work, polyester polyureas, named in the format of  $PBD_xPU_y$ , have been synthesized for the first time using a non-isocyanate route by using polyester as a soft segment. The incorporation of polyester endows toughness upon the polyureas. Hydrogen bonding between the soft and hard segments restricts the macromolecular chain folding of soft segments and decreases the crystallinity of the soft segments. The impact resistance of  $PBD_{50\%}PU_{50\%}$  reaches  $37.2 \text{ kJ/m}^2$ , which is enhanced by about four times compared to PU-10 and  $PBD_{80\%}PU_{20\%}$ . Meanwhile,  $PBD_{50\%}PU_{50\%}$  has an excellent tensile strength of 46.1 MPa and elongation at break of 135.0%. Additionally,  $PBD_{50\%}PU_{50\%}$  shows good thermal properties, with a  $T_m$  above  $180 \text{ }^\circ\text{C}$  and  $T_{5\%}$  above  $320 \text{ }^\circ\text{C}$ , which is significantly higher than its processing temperature ( $210 \text{ }^\circ\text{C}$ ). These polyureas with soft segments prepared from a non-isocyanate route possess excellent impact resistance, tensile strength and thermal properties. They have wide range of potential applications in the field of polymer materials in the future.

**Author Contributions:** Conceptualization, L.Z. and Y.L.; methodology, G.H. and L.Z.; validation, Q.X. and L.Z.; formal analysis and Y.Z.; investigation, D.S.; resources, L.Z. and Y.L.; data curation, Q.X.; writing—original draft preparation, Q.X. and L.Z.; writing—review and editing, Y.L., G.H. and B.W.; visualization, B.W., D.S. and Y.Z.; supervision, L.Z. and Y.L.; project administration, L.Z.; funding acquisition, L.Z. and Y.L. All authors have read and agreed to the published version of the manuscript.

**Funding:** This research received no external funding.

**Institutional Review Board Statement:** Not applicable.

**Data Availability Statement:** Data is contained within the article. The original contributions presented in the study are included in the article, further inquiries can be directed to the corresponding author.

**Acknowledgments:** The authors are grateful for financial support from National Natural Science Foundation of China (Grant No. 52173009), Cangzhou institute of Tiangong University (Grant No:TGCYY-F-0105), and TGU Grant for Fiber Studies (Grant No: TGF-21-A9). This project was also supported by a grant from the Program of Science and Technology Plan of the City of Tianjin (No. 24JRRRCRC00040).

**Conflicts of Interest:** The authors declare no conflicts of interest. The funders had no role in the design of the study; in the collection, analyses, or interpretation of data; in the writing of the manuscript; or in the decision to publish the results.

## References

1. Surrine, J.M.; Schexnayder, S.A.; Dennis, J.M.; Long, T.E. Urea as a monomer for isocyanate-free synthesis of segmented poly(dimethyl siloxane) polyureas. *Polymer* **2018**, *154*, 225–232. [[CrossRef](#)]
2. Wu, C.; Wang, J.; Chang, P.; Cheng, H.; Yu, Y.; Wu, Z.; Dong, D.; Zhao, F. Polyureas from diamines and carbon dioxide: Synthesis, structures and properties. *Phys. Chem. Chem. Phys.* **2012**, *14*, 464–468. [[CrossRef](#)] [[PubMed](#)]
3. Kumar, A.; Armstrong, D.; Peters, G.; Nagala, M.; Shirran, S. Direct synthesis of polyureas from the dehydrogenative coupling of diamines and methanol. *Chem. Commun.* **2021**, *57*, 6153–6156. [[CrossRef](#)] [[PubMed](#)]
4. Wolosz, D.; Parzuchowski, P.G.; Rolinska, K. Environmentally friendly synthesis of urea-free poly(carbonate-urethane) elastomers. *Macromolecules*. **2022**, *55*, 4995–5008. [[CrossRef](#)]
5. Lin, C.; Xie, K.; Tang, D. High-performance thermoplastic polyureas via a non-isocyanate route from urea and aliphatic diamines. *J. Appl. Polym. Sci.* **2022**, *139*, 52513. [[CrossRef](#)]
6. Ritter, B.S.; Mülhaupt, R. Isocyanate- and solvent-free route to thermoplastic poly(amide-urea) derived from renewable resources. *Macromol. Mater. Eng.* **2017**, *302*, 1600338. [[CrossRef](#)]
7. Jiang, S.; Cheng, H.Y.; Shi, R.H.; Wu, P.X.; Lin, W.W.; Zhang, C.; Arai, M.; Zhao, F.-Y. Direct synthesis of polyurea thermoplastics from CO<sub>2</sub> and diamines. *ACS Appl. Mater. Interfaces* **2019**, *11*, 47413–47421. [[CrossRef](#)] [[PubMed](#)]
8. Shi, R.; Jiang, S.; Cheng, H.; Wu, P.; Zhang, C.; Arai, M.; Zhao, F. Synthesis of polyurea thermoplastics through a nonisocyanate route using CO<sub>2</sub> and aliphatic diamines. *ACS Sustain. Chem. Eng.* **2020**, *8*, 18626–18635.
9. Wang, P.; Ma, X.; Li, Q.; Yang, B.; Shang, J.; Deng, Y. Green synthesis of polyureas from CO<sub>2</sub> and diamines with a functional ionic liquid as the catalyst. *RSC Adv.* **2016**, *6*, 54013–54019. [[CrossRef](#)]
10. Wu, P.; Cheng, H.; Shi, R.; Jiang, S.; Wu, Q.; Zhang, C.; Arai, M.; Zhao, F. Synthesis of polyurea via the addition of carbon dioxide to a diamine catalyzed by organic and inorganic bases. *Adv. Synth. Catal.* **2019**, *361*, 317–325. [[CrossRef](#)]
11. Wu, P.; Cheng, H.; Wang, Y.; Shi, R.; Wu, Z.; Arai, M.; Zhao, F. New kind of thermoplastic polyurea elastomers synthesized from CO<sub>2</sub> and with self-healing properties. *ACS Sustain. Chem. Eng.* **2020**, *8*, 12677–12685. [[CrossRef](#)]
12. Ying, Z.; Wu, C.; Zhang, C.; Jiang, S.; Shi, R.; Cheng, H.; Zhang, B.; Li, Y.; Zhao, F. Synthesis of polyureas with CO<sub>2</sub> as carbonyl building block and their high performances. *J. CO<sub>2</sub> Util.* **2017**, *19*, 209–213. [[CrossRef](#)]
13. Ying, Z.; Zhao, L.; Zhang, C.; Yu, Y.; Liu, T.; Cheng, H.; Zhao, F. Utilization of carbon dioxide to build a basic block for polymeric materials: An isocyanate-free route to synthesize a soluble oligourea. *RSC Adv.* **2015**, *5*, 42095–42100. [[CrossRef](#)]
14. Kébir, N.; Benoit, M.; Burel, F. Elaboration of AA-BB and AB-type non-isocyanate polyurethanes (NIPUs) using a cross metathesis polymerization between methyl carbamate and methyl carbonate groups. *Eur. Polym. J.* **2018**, *107*, 155–163. [[CrossRef](#)]
15. Kébir, N.; Benoit, M.; Legrand, C.; Burel, F. Non-isocyanate thermoplastic polyureas (NIPUreas) through a methyl carbamate metathesis polymerization. *Eur. Polym. J.* **2017**, *96*, 87–96. [[CrossRef](#)]
16. Li, S.; Sang, Z.; Zhao, J.; Zhang, Z.; Zhang, J.; Yang, W. Crystallizable and tough aliphatic thermoplastic polyureas synthesized through a nonisocyanate route. *Ind. Eng. Chem. Res.* **2016**, *55*, 1902–1911. [[CrossRef](#)]
17. Ma, S.; van Heeswijk, E.P.A.; Noordover, B.A.J.; Sablong, R.J.; van Benthem, R.; Koning, C.E. Isocyanate-free approach to water-borne polyurea dispersions and coatings. *ChemSusChem* **2018**, *11*, 149–158. [[CrossRef](#)] [[PubMed](#)]
18. Martin, A.; Lecamp, L.; Labib, H.; Aloui, F.; Kébir, N.; Burel, F. Synthesis and properties of allyl terminated renewable non-isocyanate polyurethanes (NIPUs) and polyureas (NIPUreas) and study of their photo-crosslinking. *Eur. Polym. J.* **2016**, *84*, 828–836. [[CrossRef](#)]
19. Pan, W.C.; Lin, C.H.; Dai, S.H.A. High-performance segmented polyurea by transesterification of diphenyl carbonates with aliphatic diamines. *J. Polym. Sci. Pol. Chem.* **2014**, *52*, 2781–2790. [[CrossRef](#)]
20. Jiang, Y.; Yang, S.; Pan, X. Biomass-based polyureas derived from rigid furfurylamine and isomannide. *ACS Appl. Polym. Mater.* **2022**, *4*, 2197–2204. [[CrossRef](#)]
21. Li, S.; Zhao, J.; Zhang, Z.; Zhang, J.; Yang, W. Aliphatic thermoplastic polyurethane-ureas and polyureas synthesized through a non-isocyanate route. *RSC Adv.* **2015**, *5*, 6843–6852. [[CrossRef](#)]
22. Li, H.; Cheng, H.; Zhao, F. A review on CO<sub>2</sub>-based polyureas and polyurea hybrids. *Asian J. Org. Chem.* **2022**, *11*, e202200338. [[CrossRef](#)]

23. Dennis, J.M.; Steinberg, L.I.; Pekkanen, A.M.; Maiz, J.; Hegde, M.; Müller, A.J.; Long, T.E. Synthesis and characterization of isocyanate-free polyureas. *Green Chem.* **2018**, *20*, 243–249. [[CrossRef](#)]
24. Tang, D.; Chen, Z.; Correa-Netto, F.; Macosko, C.W.; Hillmyer, M.A.; Zhang, G. Poly(urea ester): A family of biodegradable polymers with high melting temperatures. *J. Polym. Sci. Pol. Chem.* **2016**, *54*, 3795–3799. [[CrossRef](#)]
25. White, B.T.; Migliore, J.M.; Mapesa, E.U.; Wolfgang, J.D.; Sangoro, J.; Long, T.E. Isocyanate- and solvent-free synthesis of melt processible polyurea elastomers derived from urea as a monomer. *RSC Adv.* **2020**, *10*, 18760–18768. [[CrossRef](#)] [[PubMed](#)]
26. Zhang, Z.; Lin, C.; Hou, R.; Tang, D. Construction of polyallophanate vitrimers from poly(urea carbonate) via group revival induced crosslinking. *Eur. Polym. J.* **2021**, *161*, 110819. [[CrossRef](#)]
27. Zhang, R.; Huang, W.B.; Lyu, P.; Yan, S.; Wang, X.; Ju, J.H. Polyurea for blast and impact protection: A review. *Polymers* **2022**, *14*, 2670. [[CrossRef](#)] [[PubMed](#)]
28. Iqbal, N.; Tripathi, M.; Parthasarathy, S.; Kumar, D.; Roy, P.K. Tuning the properties of segmented polyurea by regulating soft-segment length. *J. Appl. Polym. Sci.* **2018**, *135*, 46284. [[CrossRef](#)]
29. Lyu, P.; Fang, Z.; Wang, X.; Huang, W.; Zhang, R.; Sang, Y.; Sun, P. Explosion test and numerical simulation of coated reinforced concrete slab based on blast mitigation polyurea coating performance. *Materials* **2022**, *15*, 2607. [[CrossRef](#)]
30. ISO 527-2:2012; Plastics-Determination of Tensile Properties-Part 2: Test Conditions for Moulding and Extrusion Plastics. International Organization for Standardization: Geneva, Switzerland, 2012.
31. ISO 178:2010; Plastics-Determination of Flexural Properties. International Organization for Standardization: Geneva, Switzerland, 2012.
32. ISO 179:2010; Plastics-Determination of Charpy Impact Properties-Part 1: Non-Instrumented Impact Test. International Organization for Standardization: Geneva, Switzerland, 2010.
33. Qi, J.; Wu, J.; Chen, J.; Wang, H. An investigation of the thermal and (bio)degradability of PBS copolyesters based on isosorbide. *Polym. Degrad. Stab.* **2019**, *160*, 229–241. [[CrossRef](#)]
34. Ai, T.; Zou, G.; Feng, W.; Ren, Z.; Li, F.; Wang, P.; Lu, B.; Ji, J. Synthesis and properties of biobased copolyamides based on polyamide 10T and polyamide 56 through one-pot polymerization. *New J. Chem.* **2021**, *45*, 14677–14686. [[CrossRef](#)]
35. Mattia, J.; Painter, P. A comparison of hydrogen bonding and order in a polyurethane and poly(urethane-urea) and their blends with poly(ethylene glycol). *Macromolecules* **2007**, *40*, 1546–1554. [[CrossRef](#)]
36. Liu, X.; Desilles, N.; Jiang, B.; Chappey, C.; Lebrun, L. High barrier semi-crystalline polyesters involving nature occurring pyridine structure towards sustainable food packaging. *Polymer* **2022**, *247*, 124790. [[CrossRef](#)]
37. Chen, M.; Saada, N.A.H.; Liu, F.; Na, H.; Zhu, J. Synthesis of copolyesters with bio-based lauric diacid: Structure and physico-mechanical studies. *RSC Adv.* **2017**, *7*, 55418–55426. [[CrossRef](#)]

**Disclaimer/Publisher’s Note:** The statements, opinions and data contained in all publications are solely those of the individual author(s) and contributor(s) and not of MDPI and/or the editor(s). MDPI and/or the editor(s) disclaim responsibility for any injury to people or property resulting from any ideas, methods, instructions or products referred to in the content.